Astron. Astrophys. 225, 143–155 (1989)

ASTRONOMY AND ASTROPHYSICS

A study of the ultraviolet spectrum of VV Cephei★

M. Hack[1], S. Engin[2], and N. Yilmaz[2]

[1] Department of Astronomy, Trieste University, Via Tiepolo 11, I-34131 Trieste, Italy
[2] Department of Astronomy, Ankara University, Besevler, Ankara, Turkey

Received July 12, 1988; accepted April 3, 1989

Summary. We have studied all the IUE images of the atmospheric eclipsing binary VV Cep (M 2 Ia e + B, $P = 20.3$ yr) available in the IUE data bank, including the period between May 5, 1978 and December 28, 1984. From the low resolution spectra we have derived $E(B-V) = 0.40$, and a good fit of the dereddened energy distribution curve with the Kurucz model for $T_{\rm eff} = 9500$ K. Moreover, comparison of the energy distribution curve with several low resolution spectra from the NASA Atlas of standard stars indicates, for the companion, a spectral type A0 II.

We have also derived the light curves after the end of the optical eclipse for wavelengths included between 1300 and 3000 Å, and have confirmed the Hagen et al. (1980) results that the opacity of the M 2 supergiant increases with decreasing wavelength.

We have identified the absorption and emission lines in the high resolution spectra. In spite of the considerable degree of reddening, no interstellar absorption lines have been detected. We have shown the presence of slight stratification effects, indicated, for instance, by systematic differences in radial velocity relatively to the Fe II absorption lines of Mg I 2852, of the Mg II resonance doublet, and of the semipermitted emission line 1641 0 I]. These effects become more evident at phases just following the end of the eclipse.

Key words: stars: binaries: VV Cephei – ultraviolet spectrum

1. Introduction

We have collected all the IUE images of the atmospheric eclipsing binary VV Cep (M 2 I ae + B) available in the IUE data bank, in order to study the spectral type of the hot companion and the spectral variations following the end of the eclipse.

The observations cover the period included between May 5, 1978 and December 28, 1984. The third contact, according to optical observations, occurred between February 18 and March 10, 1978, and the fourth contact by May 20 (Hagen et al., 1980).

A study of the low resolution spectra taken between April 1, 1978 and May 1979, and of a few high resolution spectra (one SWP image of April 1, 1978, and some LWR images obtained between April 1978 and May 1979) has been made by Hagen et al. (1980). We have obtained a confirmation of their results from the low resolution spectra, and we have made a detailed study of all the high resolution images.

One of the purposes of this study was to derive the spectral type of the hot component. Optical observations, because of the contributions of the M 2 Ia primary and of the rarefied envelope surrounding the primary or the whole system, give very uncertain results. In fact, the spectral types assigned to the companion from optical studies range between O and A.

2. The low resolution spectra

Tables 1a and 1b give the list of the low and high resolution spectra respectively. The phases have been computed by the relation Epoch of minimum = 2443360 + 7430 E (Kholopov, 1985).

2.1. *Flux variation versus Julian day at various wavelengths*

As already observed by Hagen et al. (1980), the atmospheric eclipse ended later in the ultraviolet than in the optical range. According to them, the integrated near ultraviolet flux reached the almost constant value expected at the end of eclipse, at the beginning of July 1978, while the integrated far ultraviolet flux reached the out-of-eclipse value at the end of July 1978.

We have traced the continuum passing through those regions of the spectrum where no strong emission or absorption features are present. In Fig. 1 we have plotted the flux in erg s^{-1} cm^{-2} $Å^{-1}$ versus the JD. The epoch of the fourth contact falls on JD 2443900 (Jan. 26, 1979) at 1300 Å, on JD 2443800 (October 18, 1978) between 1400 and 2300 Å, and on JD 2443750 (August 29, 1978) between 2800 and 3000 Å. It is evident that the opacity of the M 2 supergiant atmosphere increases rather regularly toward shorter wavelengths. Also the amplitude of the observed part of the light curve depends on the wavelength, varying between $\Delta m = -1.36$ at 1240 Å, reaching a maximum of -3.3 between 1500 and 1700 Å, and then decreasing to -1.5 and remaining constant between 2500 and 3000 Å. This behavior reflects the combined effects of the wavelength dependence of the opacity of the eclipsing body and of the energy distribution of the eclipsed companion. It is possible that a contribution to the changing magnitude difference with wavelength may be ascribed to the photoionized region; however, as we shall see in the following, the

Send offprint requests to: M. Hack

★ Based on data obtained from the IUE Data Bank at the Villafranca Satellite Tracking station. The data analysis has been performed at the ASTRONET pole of the Trieste Astronomy Department and Astronomical Observatory.

temperature of the companion is too low to produce an important effect of this type.

2.2. Determination of the interstellar extinction

We have used the low resolution spectra from 1200 to 3000 Å to derive the interstellar reddening and therefore obtain a determination of the corrected energy distribution, and thus the spectral type of the companion.

The continuum fluxes were averaged over a 40 Å region, and then a continuous line was traced through the highest points of the spectrum, where no emission lines were present. The spectra obtained between Oct. 1979 and Feb. 1982 with the large aperture do not show any difference from one another that are larger than the errors one makes in tracing the continuum through the highest points of one and the same spectrum. Hence we have averaged the fluxes derived from these spectra. The relative standard deviations s/F range from 6 to 10%. Error bars transformed into the logarithmic scale of the graph in Fig. 2 range from ± 0.09 to ± 0.02. We have applied the relation

$$\log F_{corr} = \log F_{obs} + 0.4\, k_\lambda\, E(B-V) \quad \text{(Jamar et al., 1976)}$$

to this average spectrum, for values of $E(B-V)$ included between 0.30 and 0.47. The depression at 2200 Å disappears for $E(B-V) = 0.40$. As a check on the reliability of this value, we have considered several stars in the same region of VV Cep (Table 2) observed with the satellite TD 1 (Jamar et al., 1976). Figure 3 shows the relation between the observed $E(B-V)$ vs. the distance modulus M_v-V (M_v from the spectral type, see Allen, 1973). This relation shows that a value of $E(B-V)$ of 0.40 ± 0.05 is very reasonable. This value is higher than that of 0.30 derived by Wawrukiewicz and Lee (1974) from the optical spectrum. Their value will fit the relation in Fig. 3 if we assume that the luminosity class of VV Cep is II rather than Ia. We will discuss this point in the next section. However, for $E(B-V) = 0.30$ the depression at 2200 Å is still clearly present. We cannot exclude that this depression is only apparent and due to the combination of the spectrum of the hot star and a Balmer continuum produced by

Table 1a. The low resolution images

SWP	A	J.D. 244	Phase	Exp. m s	LWR	A	J.D. 244	Phase	Exp. m s
1405	S	3622	0.035	4	1285	L	3607	0.033	20
	L			20	1452	S	3636	0.037	1
1501	L	3636	0.037	15		L			1 30
1588	S	3649	0.039	10	1524	L	3649	0.039	30
	L			31	1631	S	3667	0.041	4
1736	S	3667	0.041	1		L			6
	L			12	1750	S	3690	0.044	2 30
1883	S	3690	0.044	8		L			5
	L			15	1808	S	3700	0.046	1
1957	S	3700	0.046	10		L			1
	L			15	2487	S	3780	0.057	1
2162	S	3721	0.048	1		L			1
	L			2	2885	S	3822	0.062	1
2342	L	3741	0.051	15		L			1
2796	S	3780	0.057	7	3271	S	3868	0.068	1 30
	L			10		L			1
3276	S	3822	0.062	20	4242	S	3975	0.083	1 30
	L			2 30		L			1
3321	S	3825	0.063	7	4244	L	3975	0.083	5
	L			10	4523	S	4009	0.087	1 30
3699	S	3868	0.068	18		L			1 30
	L			3	6664	S	4254	0.120	1 14
3887	L	3885	0.071	2 30		L			2 30
4617	S	3946	0.079	30	8139	S	4419	0.143	1
	L			1 30		L			2 30
4919	S	3975	0.083	10	10030	L	4662	0.175	2
	L			1 30	10809	S	4764	0.189	10
5240	S	4009	0.087	12		L			2 30
	L			3	12538	L	4939	0.212	2 30
6821	L	4157	0.107	3					
7217	S	4203	0.113	9 59					
	L			2 29					
7655	L	4254	0.120	7 29					
9389	S	4419	0.143	10					

Table 1b. The high resolution images

SWP	A	J.D. 244	Phase	Exp. m s	LWR	A	J.D. 244	Phase	Exp. m s
1725	L	3665	0.041	180	1373	L	3622	0.035	40
2140	L	3719	0.048	80	1374	L	3622	0.035	30
3322	L	3825	0.063	270	1525	L	3649	0.039	30
3888	L	3885	0.071	120	1673	L	3675	0.042	60
4575	L	3943	0.079	120	1807	L	3700	0.045	45
5241	L	4009	0.087	75	1931	S	3721	0.049	113
5907	L	4078	0.097	199 59	2109	S	3739	0.050	120
7218	L	4203	0.113	119 59	2886	L	3822	0.062	45
7657	L	4254	0.120	110	2923	L	3825	0.063	30
9390	L	4419	0.143	120	2924	L	3825	0.063	60
13374	L	4663	0.175	120	3272	L	3868	0.068	30
13383	L	4664	0.176	300	3896	L	3933	0.077	40
14220	L	4764	0.189	90	4243	L	3975	0.083	30
14221	L	4764	0.189	164	4524	L	4013	0.088	30
20090	L	5483	0.286	75	5804	L	4157	0.107	24 59
24770	L	6064	0.364	100	6221	L	4203	0.113	29 59
					6665	L	4254	0.120	29 59
					6666	L	4254	0.120	54 59
					8140	L	4419	0.142	30
					8141	L	4419	0.142	120
					10031	L	4663	0.175	15
					10032	L	4663	0.175	190
					10037	S	4664	0.175	25
					10810	L	4754	0.189	22
					10811	L	4754	0.189	22
					10812	L	4754	0.189	45
					12539	L	5010	0.222	210
					12540	L	5011	0.222	30
					12541	L	5011	0.222	15
					16277	L	5517	0.290	10

the photoionized region surrounding the hot star or the whole system.

To check this, we have compared our spectrum – de-reddened for $E(B-V)=0.30$ and 0.40 – with a spectrum obtained by adding the dereddened flux of the M 2 Ia b star α Ori, $E(B-V)=0.21$ to the flux of the B9.5 III star Delta Cyg, $E(B-V)=0.02$, or to that of the A0 II star HD 111775, $E(B-V)=0.03$ (IUE data, Kalinowski, 1983). This was done after having divided the flux of α Ori by a factor such that $V(\alpha\,\text{Ori})-V(\text{hot star})$ becomes equal to the difference in visual magnitude between VV Cep A and VV Cep B: $V(\text{M})=5.25$ and $V(\text{companion})=6.97$ (Peery, 1966). The contribution of the M supergiant is completely negligible in the whole IUE spectral range. The agreement of the spectrum of VV Cep dereddened for $E(B-V)=0.40$ with the spectrum of the A0 II star HD 111775 is very good (Fig. 4), the largest discrepancies being less than the error bars affecting the average continuum. Hence, it seems reasonable to admit that the contribution of the hydrogen bound-free continuum is negligible.

Comparison of the spectrum of the companion with other B8 or A1 stars shows clear disagreement. Hence the best fit is obtained with a spectral type A0 II. This result strongly disagrees with that of Warukiewicz and Lee (1974), who, from optical photometric measurements derived a spectral type B1, 2 V. Instead our result is in good agreement with that found by Faraggiana and Selvelli (1979) from one low resolution IUE spectrum.

We have also compared the spectrum dereddened for $E(B-V)=0.40$ with the Kurucz (1979) models, obtaining a good fit for $T_{\text{eff}}=9500$ K. The effect of the opacity of the eclipsing body is detectable in all the spectra obtained during the period May 7 to July 31, 1978 (Fig. 5). These spectra, even after correction for interstellar extinction, present an energy distribution curve which cannot be fitted with that of any standard star or any Kurucz model, and are characterized by a broad depression between about 1300 Å and 2000 Å. This depression cannot be explained with blends of the absorption lines, because, as we shall see in Sect. 3, the high resolution spectra do not show any appreciable absorption line variation during the period May 1978 – December 1984.

2.3. *Absolute magnitude of VV Cephei A*

We have applied the Wilson-Bappu relation for deriving the absolute visual magnitude of VV Cephei. Measurements of the width of the *H* and *K* emission lines, using several high resolution (9 and 12 Å mm^{-1}) optical spectra obtained at the 193 and at the

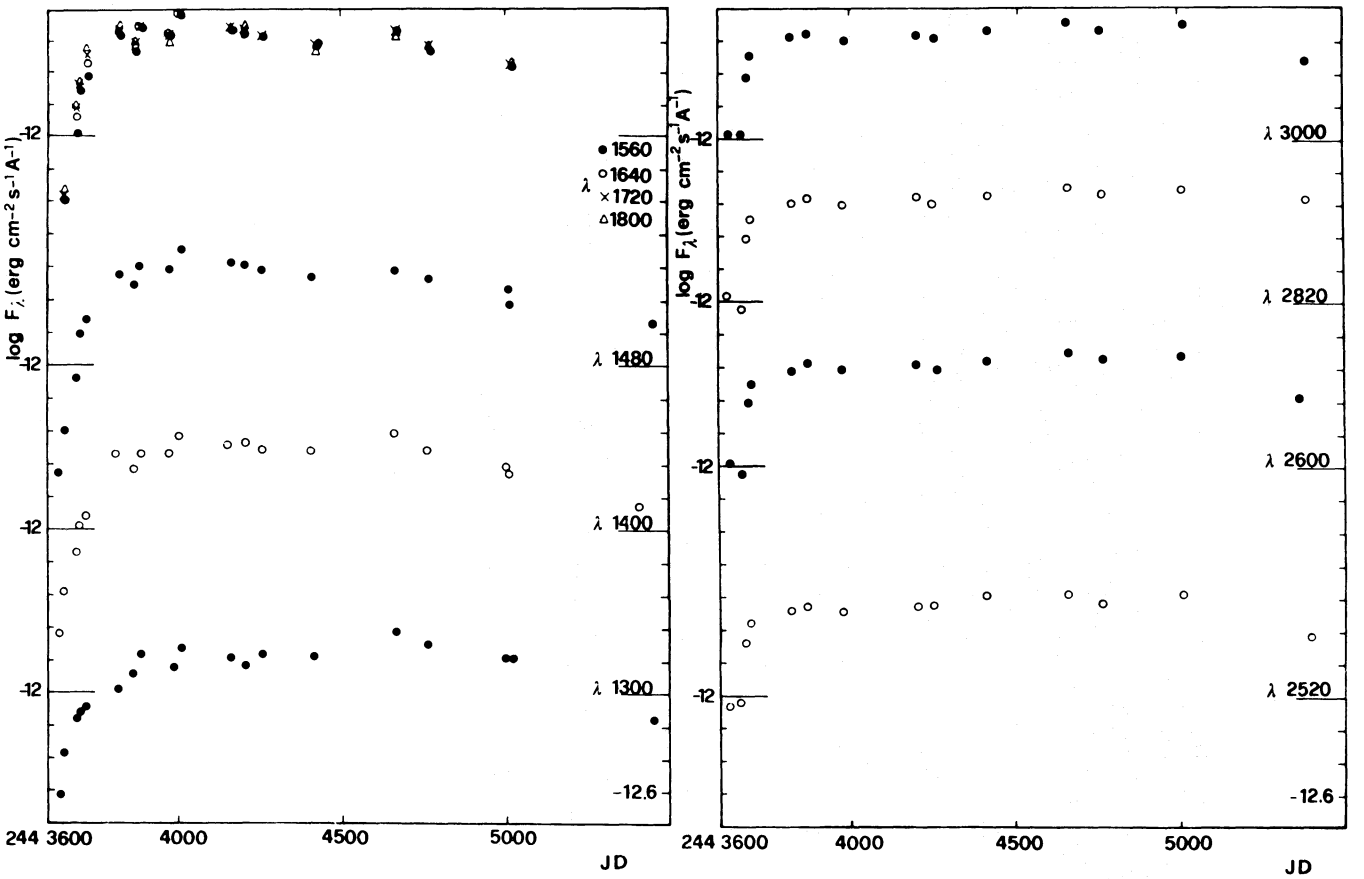

Fig. 1. log F_λ (erg cm^{-2} s^{-1} Å^{-1}) vs. JD for wavelengths between 1300 Å and 3000 Å

152 telescopes of the Haute Provence Observatory (work in progress) give $M_V = -7 \pm 1$. This measurement has been made only for 4 spectrograms, where the two emission wings are stronger than the continuum. In the majority of the spectrograms the emission wings cut the absorption wings of the photospheric line and are well below the continuum, or else just one wing is detectable. In all these cases the determination of the width of the *K* emission is very uncertain or impossible.

We have also used the width-luminosity relationship for the Mg II *k* line (Elgaroy, 1988). The widths of the Mg II *k* emission line have been measured on the high resolution spectra (Table 3). The relation derived by Wiler and Oegerle (1979) between the line width measured at the base of the emission line and M_v gives $M_v = -4$. Another relation found by Vladilo et al. (1987) between the FWHM and M_v gives $M_v = -6.49$. This value is an upper limit for the luminosity, because we have measured the width at half maximum intensity, assuming that the maximum of the emission wings is the maximum of the total emission, which, however, is cut by a strong absorption. Hence our FWHM is an upper limit to the true value. In conclusion, if we assume the more probable value for $M_v = -6.5$, we find, for the companion, $M_v = -4.8$, corresponding to a luminosity class Ib-II.

If, on the contrary, we assume $M_v = -4$, the absolute magnitude of the companion becomes equal to -2.3, corresponding to a luminosity class II-III.

Elements in favor of the higher luminosity are: the persistence of the depression at 2200 Å for $E(B-V) = 0.30$, and the indication given by the Wilson-Bappu relation for the Ca II emission lines.

In spite of the relatively high reddening, no interstellar absorption lines are detectable in the high resolution spectra, with the possible exception of the C I and O I resonance lines. However, also non resonance lines of C I are present, and they may be formed in the outer atmospheric layers of the M supergiant. Several strong resonance lines of once ionized elements are probably a blend of photospheric, circumstellar and interstellar components. Resonance lines of neutral elements (like those of C I, O I and Mg I) may be due partly to interstellar and partly to circumstellar absorption or even to absorption from an extended outer atmosphere of the M 2 supergiant.

2.4. The Ly α emission line.

We have measured the flux of the Ly α emission in the low resolution spectra, because, unlike the high resolution spectra, it is probably affected in a negligible way by the geocoronal contribution. In fact, the exposure times are short and always equal to or less than 20 minutes, with only one exception (SWP 1588, large aperture, exposure 31 minutes, which, however, gives a rather low value of Ly α flux).

Table 4 gives the flux in erg cm^{-2} s^{-1} contained in the whole line. The values are obtained from the spectra taken with the large aperture. It is interesting to note that spectra obtained almost simultaneously, with the small aperture, do not show any measurable Ly α emission. We think that this is due to the fact that the

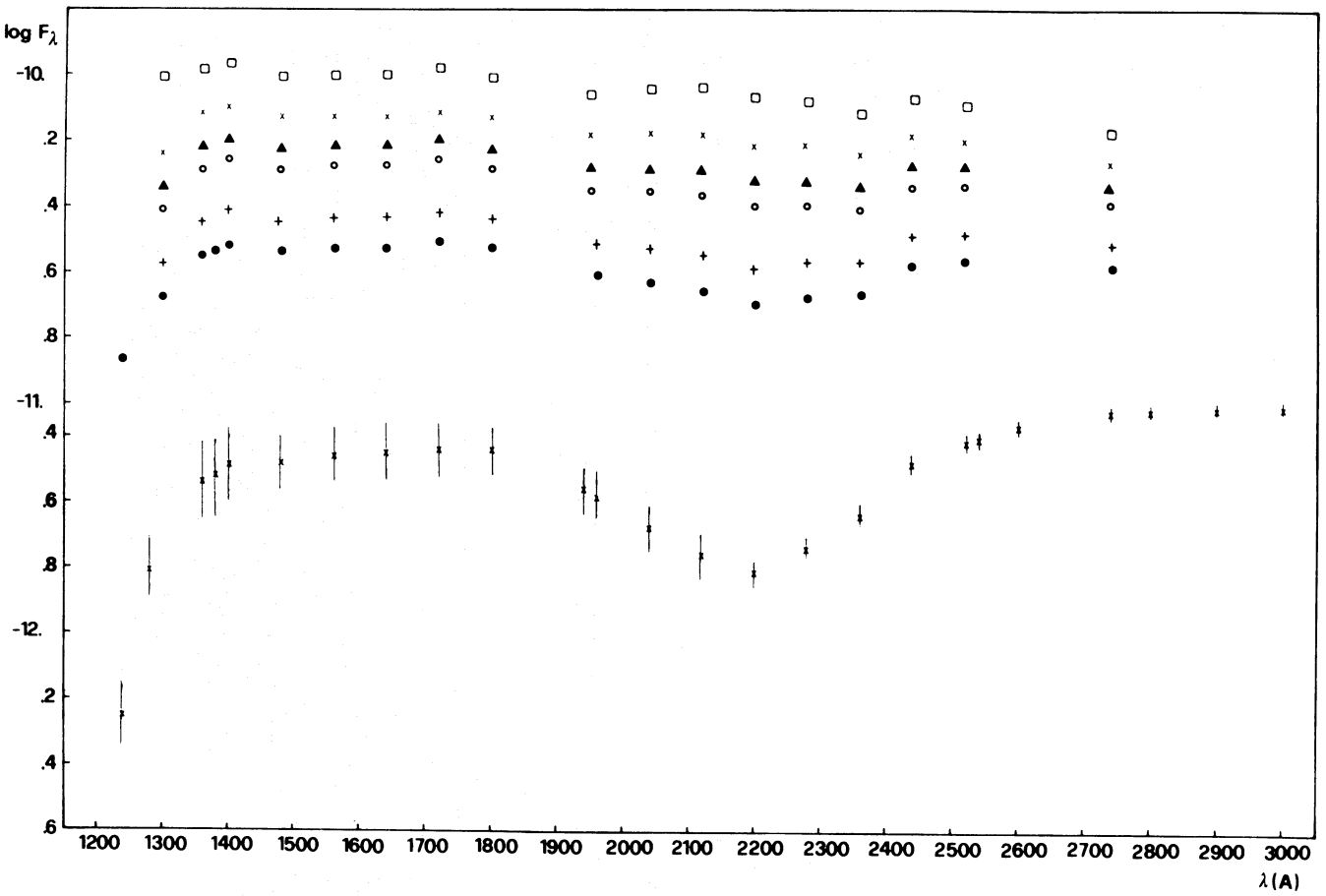

Fig. 2. The bottom graph (×) gives the average of the spectra from May 1979 to February 1982, not corrected for reddening. The upper graphs give the spectra dereddened for $E(B-V)=0.30$ (●), 0.33 (+), 0.38 (○), 0.40 (▲), 0.43 (×) and 0.47 (□)

Table 2. Stars in the same angular region of VV Cephei

Star	R.A.(2000)	Dec.(2000)	$E(B-V)$	$M-m$
VV Cep	$21^h56.^m7$	+63° 37′		
HD 206267	21 38.9	57 29	>0.35	−11.6
206773	21 42.4	57 44	0.51	−11.0
208095	21 52.0	55 48	0.01	− 6.4
208682	21 55.5	65 20	0.15	− 8.5
208947	21 57.2	66 10	0.18	− 9.3
208905	21 57.3	61 17	0.01	− 6.4
209339	22 00.7	62 29	0.37	−11.4
14 Cep	22 02.1	58 00	0.38	−10.7
209744	22 03.9	59 49	0.48	−10.2
19 Cep	22 05.1	62 17	0.36	−12.1
210071	22 06.2	56 20	−0.06	− 6.6
λ Cep	22 11.5	59 25	>0.35	−11.05
211242	22 13.8	63 10	0.02	− 6.15
212454	22 23.0	57 17	−0.03	− 6.35
26 Cep	22 27.1	65 08	0.59	−11.5

emission is formed in the envelope surrounding the system. Indeed, even when the exposure obtained with the small aperture is much longer (up to 6 times, as for SWP 3699, or 8 times as for SWP 3276) than that obtained with the large aperture, the Ly α is not detectable at all.

The observed irregular variations may be real, at least for the best exposed spectra, since they are larger than 50%, while the photometric errors at 1200 Å can be estimated at 20%.

3. The far-ultraviolet high resolution spectra

Table 1b gives the image numbers, dates and exposures of the high resolution spectra which have been studied.

The far ultraviolet high resolution image obtained during the last phase of the atmospheric eclipse (June 1978) does not show any appreciable difference from the images obtained later on, from 1979 to December 1984, except for the value of the continuous flux. The spectrum is dominated by a large number of absorption lines of the ions given in Table 5. Only a few emissions are present: a) the Ly α, which probably receives an important contribution from the geocoronal line, since all the exposures are longer than one hour; b) the O I triplet at 1302–1306 Å, O I 1325 Å (doubtful), O I] 1641 Å; c) the metastable line of N I at 1745 Å,

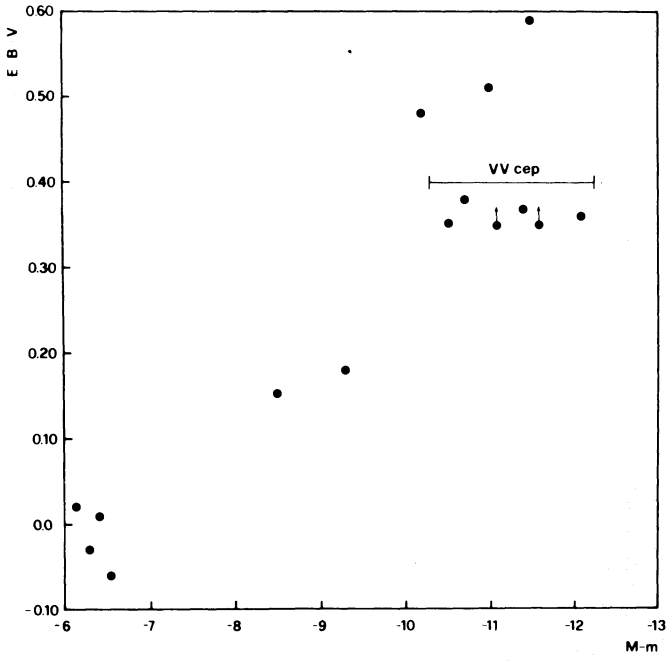

Fig. 3. $E(B-V)$ versus M − m for stars in the same angular region as VV Cep

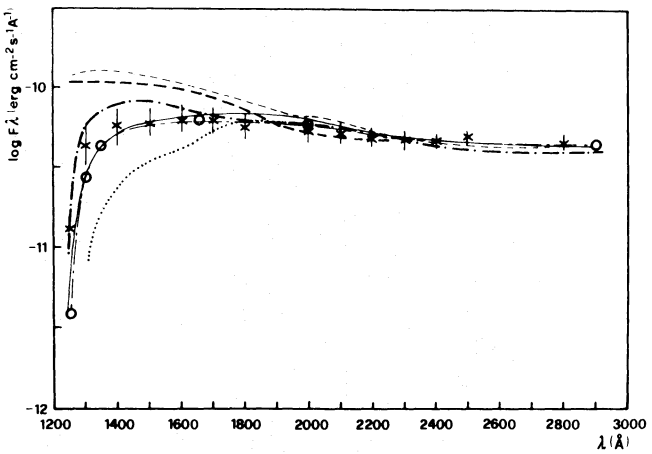

Fig. 4. The out-of-eclipse average spectrum of VV Cep dereddened for $E(B-V)=0.40$ (- - - × - - - with error bars) compared with unreddened standard stars of different spectral types: — — — HD 46769 B8 Ib; - - - - - - HD 10205 B8 IV; – · – · – Delta Cyg B9.5 III; o – · – · – · HD 111 775 A0 II; - - - - - - - - HD 103287 A0 V$^+$; ..... HD 166205 A1 V

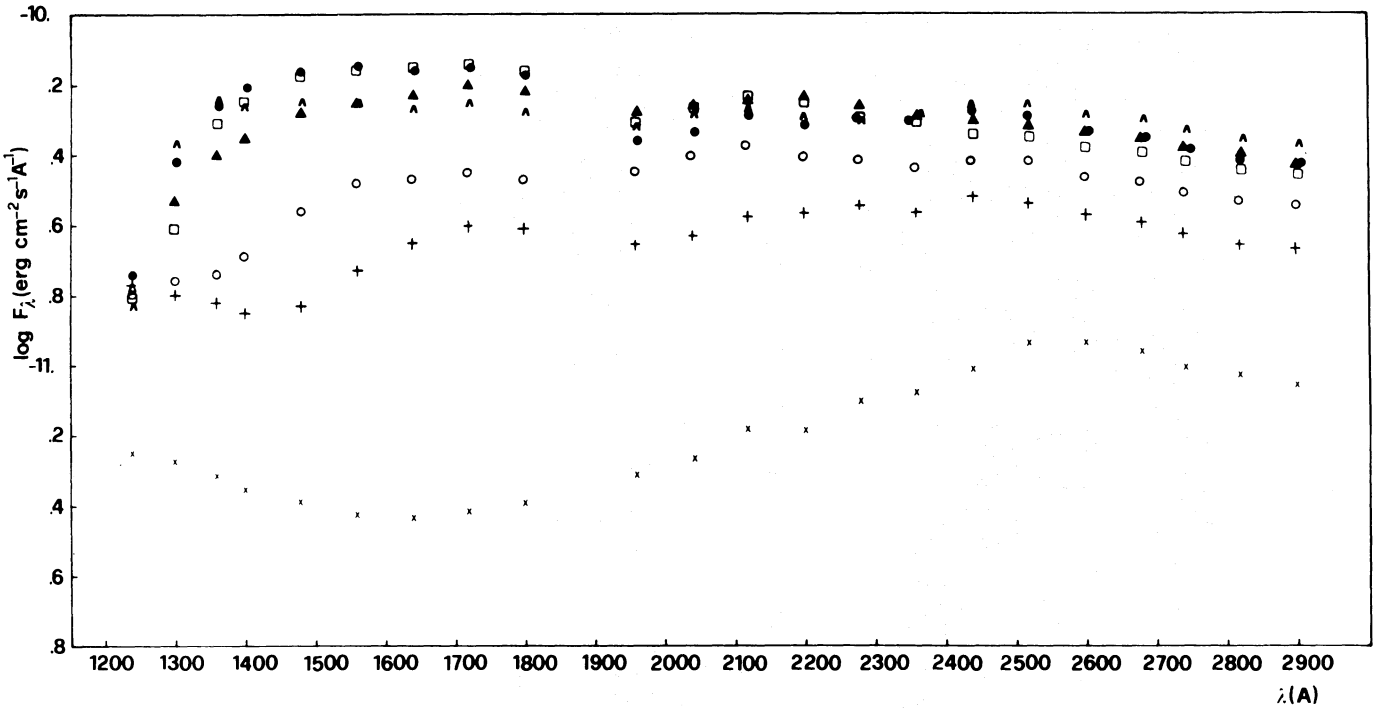

Fig. 5. The spectra de-reddened for $E(B\text{-}V)=0.40$: x May 7, 1978; + June 30, 1978; o July 10, 1978; □ November 9, 1978; ▲ December 25, 1978; ● average of spectra obtained on October 10, 1979, November 25, 1979, January 1980 and June 28, 1980; Λ average of spectra of February 26, 1981, June 8, 1981 and February 9–10, 1982

Table 3. Width (km s^{-1}) of the Mg II *k* line

Image LWR	Full width at the base	FWHM
1525	456	
1673	470	
1807	500	
2109	358	
2886	358	
2923	358	
2924	370	
3272	310	
4007	369	
4243	357	
4524	335	
5804	322	
6665	357	
6666	357	
8140	369	
8141	389	
10031	394	298
10032	429	294
10811	366	278
10812	402	295
12541	389	281
16276	428	300
16277	334	298
Mean	382	292
s	47	2

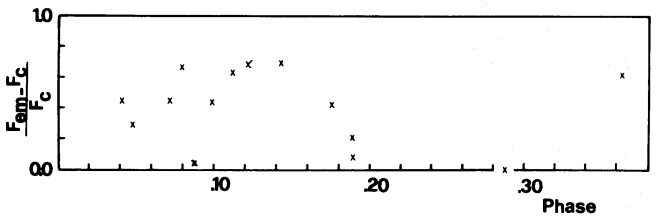

Fig. 6. Central intensity $(F-F_c)/F_c$ for 1869.5 Fe II versus the phase

while the other line of the same multiplet, at 1742 Å, is absent or present in absorption; d) the Fe II multiplet 191 at 1785–1787 Å, and e) an emission at 1869 Å which has been identified by Johansson and Jordan (1984) with one Fe II fluorescent line pumped by Ly α. The intensities of all these lines relative to the nearby continuum fluctuate irregularly, but the percentage variation is less than 18% and is probably not real but due to the uncertainties by which the continuum is traced. Only 1869 Å seems to present real variations, reaching a flux of about 1.7 times the nearby continuum at phases 0.08–0.14 and almost disappearing at phases 0.19 and 0.29 (see Fig. 6 and 7c). The transitions to $b^4\,G$, besides 1869.55 Å, which is the strongest line, include also the line at 1872.64. It is impossible to say if this line is present and behaves in the same way as 1869.55, because of the presence of a resau mark just at that wavelength.

The emission lines present in the far UV need some discussion. O I: the strongest permitted lines of the triplet at 1302, 1304 and

Table 4. Total intensity of Ly α

SWP images (low resolution large aperture) and phases		Total flux (10^{-12} erg cm^{-2} s^{-1})
1501	0.037	3.6
1588	0.039	5.6
1883	0.044	8.9
1957	0.046	4.2
2162	0.048	4.2
3276	0.062	5.9
3699	0.068	14.1
3887	0.071	Ly α not detectable
4919	0.083	Ly α not detectable
5240	0.087	4.2
6821	0.107	2.1
7217	0.113	17.2
7655	0.120	5.4
9389	0.143	7.4
13373	0.175	24.1
14219	0.189	19.3
16300	0.222	20.7
16302	0.222	7.4

1306 Å seem to exhibit a P Cygni profile. However the absorption component, falling at rest wavelength, may be of interstellar origin (Fig. 7a). The emissions have an intensity ratio very different from the theoretical one (1302:1304:1306 = 5:3:1) and they are fainter than the semipermitted line at 1641 Å (Table 6). It must be noted that the intensity of 1302 is uncertain because the line is partially affected by the presence of a resau mark, and 1304.86 is close to the absorption line of Si II at 1304.41. However we must explain why 1641 is about 3 times stronger than 1306. The same effect was observed for the symbiotic star CH Cygni by Hack and Selvelli (1982). They have interpreted it as an indication that the physical conditions in the envelope are far from the optically thin case. Large optical thickness means that the 1302–1306 photons will scatter many times before eventually escaping from the neutral oxygen region. If the scattering number is very high, processes with a small probability per scattering of destroying resonance lines can become important (Hummer, 1968; Osterbrok, 1962). This fact will explain the anomalous line ratio, because the 0.00 eV level is more populated and, therefore, after many scatterings, substantial reabsorption will occur and the 1302 emission will be weaker; the 0.04 eV level is less populated, and therefore the 1306 line will be less reabsorbed and the emission will be stronger. There is a small but finite chance that at each coherent resonance scattering, decay from the upper term $3s^3\,s^0$ will occur through the 1641.3 intersystem line $3s^3\,S^0 \rightarrow 2p^4\,{}^1D$ that shares the upper term with the 1302–1306 lines.

Another possibility is that the anomalous intensity ratio may be due to interstellar absorption, which, if present, would be stronger at 1302 and missing at 1641.

The metastable line of N I 1745.249 Å ($\log gf = -1.03$) is found in emission, while the stronger line of the same multiplet, at 1742.737 Å ($\log gf = -0.63$) is in absorption, and the lines at

Table 5. Ions detectable in the far UV spectrum

C I: ground level multiplets 2, 3, 4, 5, 6, 7 and excited multiplets 33, 34, 35, 36, 37, 38, 39, 40, 41, 42, 43, 47, 48, 49, 50, 51, 52, 53, 54, 62, 63, 64, 65
C II: multiplet 1, 10, 11, 14
C III: multiplet 9
C IV: multiplet 1
N I: excited multiplets 4, 5, 12 in absorption, 1745.25 multiplet 9 in emission, while 1742.73 same multiplet in absorption
N V: multiplet 1 possibly present, but doubtful because at 1240 the continuous flux is almost zero
O I: multiplet 2 in emission, semipermitted multiplet 1 in emission (very weak) and semipermitted line at 1641 in emission (rather strong)
Mg II: the strongest line in this spectral range, 1753.4744, i = 500 (1737.6238, i = 500 is blended)
Al II: the resonance line at 1670.787 and possibly the strongest line of multiplet 4, 1862.311 (blended with Al III) and of multiplet 5 (1763.952 + 1763.869 blended with Fe II)
Al III: multiplet 1
Si II: multiplets 1, 2, 3, 4, 7, 11, 13, 15
Si III: multiplets 3, 4, 10, 20, 36, 38, 39, 46, 52, 58, 60, 61, 66, 67
Si IV: multiplet 1
P II: multiplet 1 and, possibly multiplets 2 and 3 in blends
P III: multiplet 1
S II: multiplet 1
Ti II: ground level multiplet 3
Ti III: ground level multiplets 1, 2, low excitation multiplets 4 and 5
V II: multiplets 18, 19, 58, 59, 80, 106, 116, 127, 128, 138, 139, 163, 195 and the strong ground level line at 1828.84 (i = 500)
Cr II: multiplets 31, 33, 39, 40, with i > 400
Mn II: multiplets 10, 11, 12, 13
Fe II: all the lines with intensity > 1 and low EP < 5 eV are present; multiplet 191: the lines have two emission wings
Fe III: missing
Co II: multiplet 5
Ni II: all the ground level lines (multiplets 1–10) are present, and several low excitation lines may be present in blends

Note: All the wavelengths, intensities and multiplets are from Kelly (1987).

1492.626 Å (log $gf = -0.46$) and at 1494.676 Å (log $gf = -0.71$) from the same upper level are in absorption (the log gf are from Kurucz, 1975). The only possible explanation for this behavior of the N I lines is that 1745, which is the faintest in the group, does not present self-absorption, while the other three do (Fig. 7b).

The multiplet 191 of Fe II is often observed in emission in several stars with extended envelopes, because it has the upper level in common with the resonance multiplet 9 at 1260 Å, and since the f values of the lines of multiplet 191 are much stronger than those of multiplet 9, multiplet 191 is favored in recombination (Fig. 7d).

The absence of any variation in intensity of the absorption lines (both from ground and excited levels) of neutral elements, like C I and N I, which, if formed in the atmosphere of the M supergiant, should be filled by the hot continuum of the companion, indicates that they originate in the circumstellar envelope.

4. The near ultraviolet high resolution spectra

The near ultraviolet high resolution spectra are dominated by the absorption lines of once ionized metals, Ti II, V II, Cr II, Mn II and especially Fe II. The Mg II resonance doublet present two emission wings with varying R/V ratio (Fig. 8). Both the resonance absorption components of Mg II and the resonance absorption line of Mg I have no flux left at their center along the whole period of observation. Hence they are formed in the circumstellar envelope, because they are not filled by the continuum of the hot companion. No evidence of interstellar components is detectable in these strong lines. However, if present, they should be blended with the circumstellar components.

Besides the emission wings of Mg II at 2795 and 2802 Å, few other emissions of Fe II are present (see Table 7). The strongest one is a blend of Fe II (Mult. 391) at 2839.513 Å and Fe II (Mult. 380) at 2839.799, which does not show an absorption component. Other moderately strong emissions are Fe II (Mult. 373) at 2845.450 Å, also without an absorption component, and Fe II (Mult. 373) at 2785.192 Å with a weak absorption and strong emission wings. The levels $e^4\,D$ and $e^6\,D$ (upper levels of multiplets 363, 373, 380, 391, 399) are known to be overpopulated with respect to the lower levels, although the mechanisms which overpopulate these high excited states are not well understood. This explains why we observe in emission $\lambda\lambda$ 2839, 2845 and 2785 Å, which are the strongest lines of these multiplets.

The strongest lines of multiplets 60, 62 and 78 present two emission wings: the two semi-permitted lines at 2926.586 and 2953.774 Å of Fe II], multiplet 60; Fe II 62 at 2755.734 Å, Fe II 78 at 2984.824 Å and at 3002.650 Å. Multiplets 60, 62 and 78 have upper levels which are respectively $z^6\,F$, $z^4\,F$ and $z^4\,P$ which are the lower levels of multiplets 373, 391 and 181 optical (whose upper levels is $e^4\,D$) respectively, and which could be overpopulated by the levels $e^4\,D$ and $e^6\,D$, thus explaining the observed emission wings.

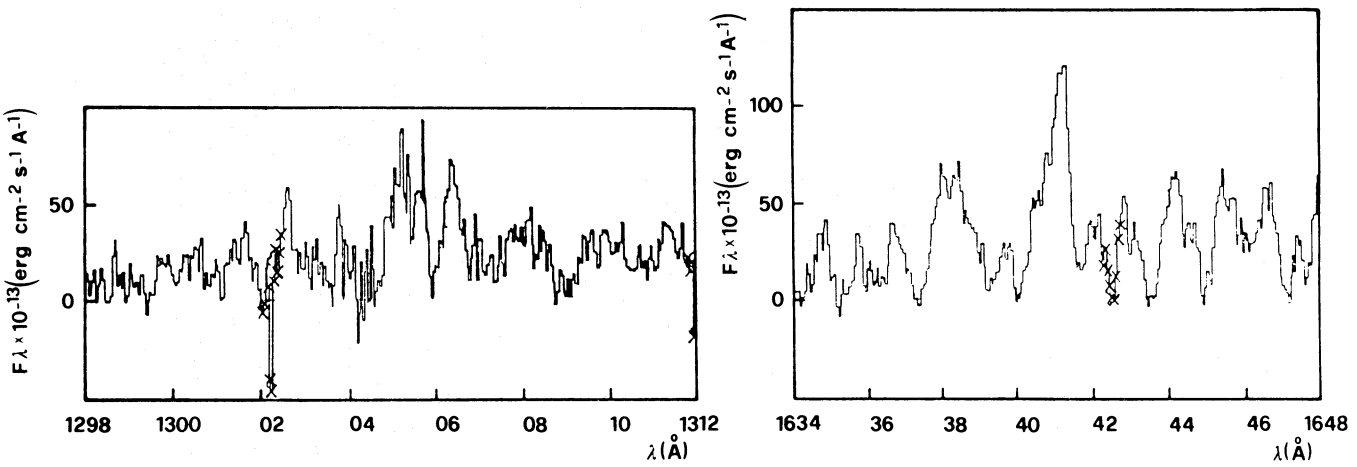

Fig. 7a. 1302.17, 1304.86 and 1306.02 O I and 1641.3 O I]

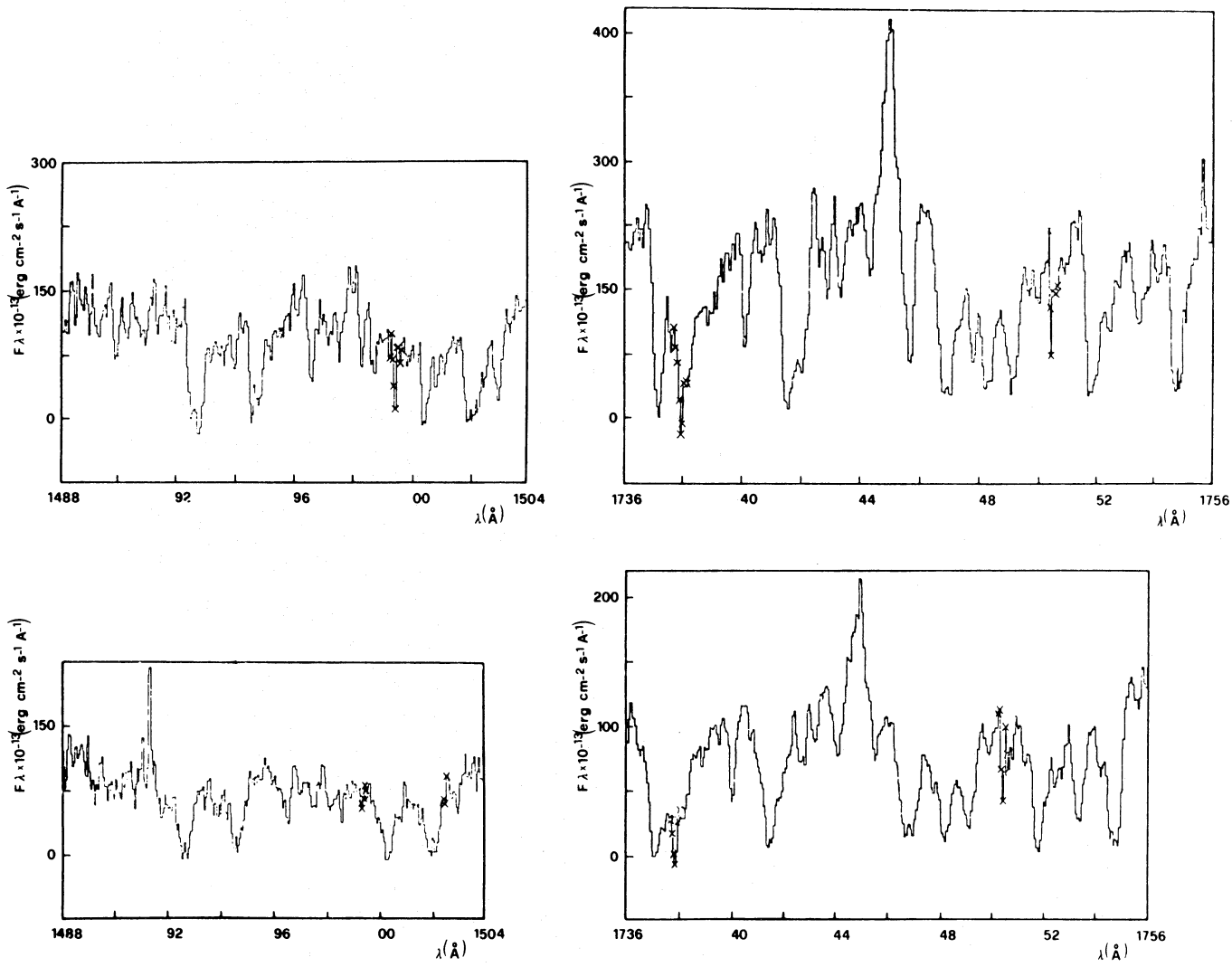

Fig. 7b. N I lines at 1492.63, 1494.67 and at 1742.74, 1745.26; top phase 0.11, bottom phase 0.19

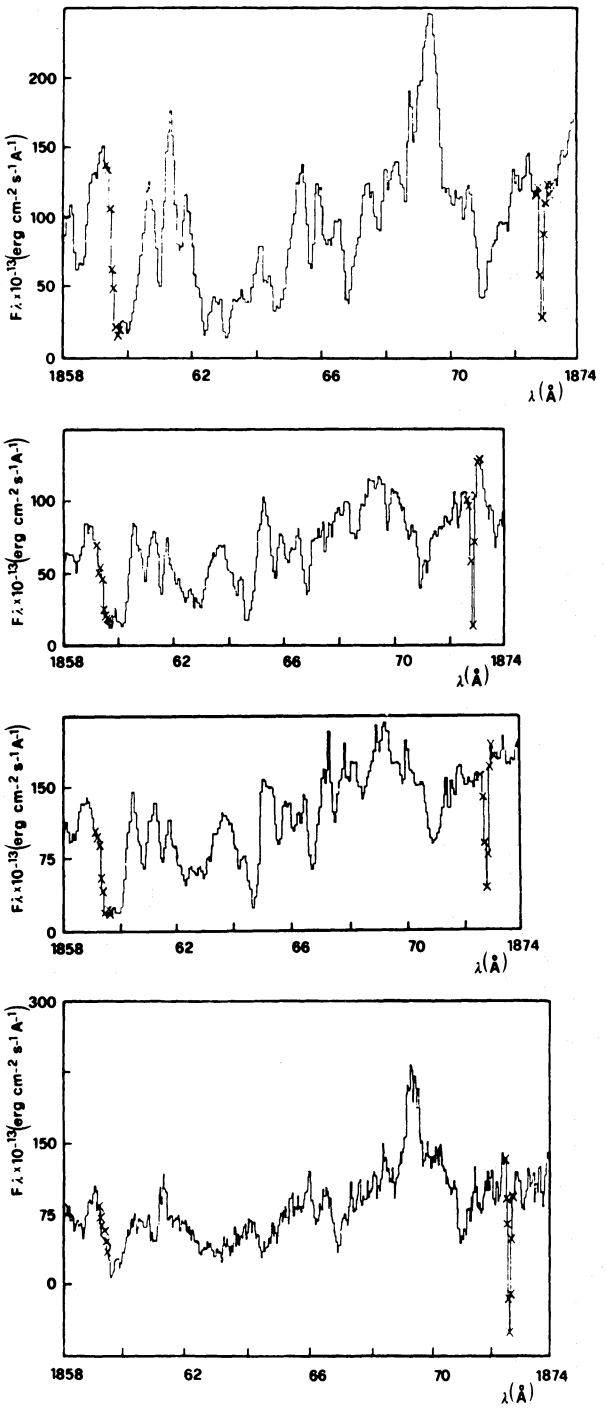

Fig. 7c. 1869 Fe II; from top to bottom: phase 0.11, phase 0.19 (SWP 14220), phase 0.19 (SWP 14221), phase 0.36

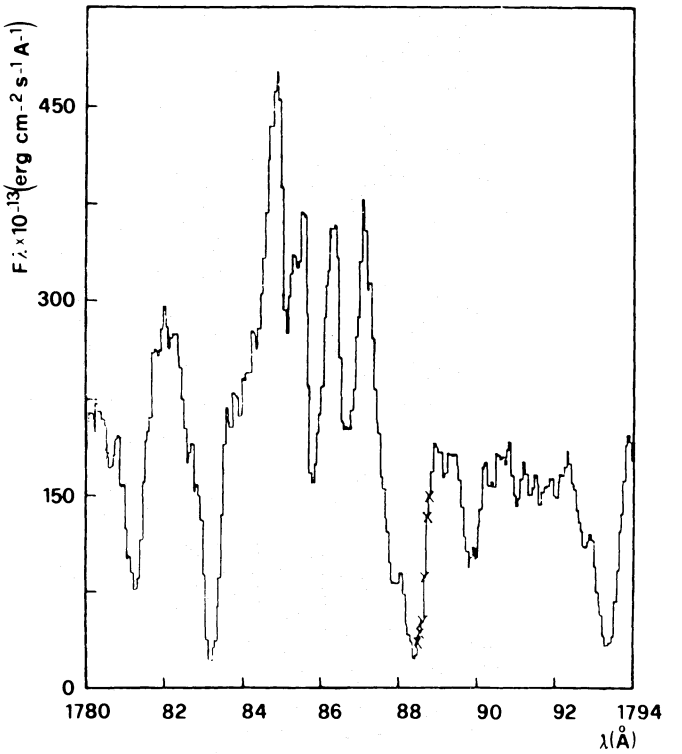

Fig. 7d. Fe II multiplet 191

Also the near ultraviolet region does not present any appreciable variation in the spectral features, with the exceptions of the flux in the emission wings of Mg II and their ratio R/V (Fig. 8 a, b, c) and the intensity of the strongest emissions in the near UV spectrum, 2839 and 2756 Fe II. Figure 9 shows their intensities, measured relatively to the nearby continuum, versus the phase. Both the central intensity of 2869 and the two emission wings of 2756 decrease regularly from phase 0.04 to phase 0.29.

Table 6. Average fluxes (erg $cm^{-2} s^{-1} Å^{-1}$) of the O I emission lines and standard deviations

λ	$F \times 10^{-13}$	$s \times 10^{-13}$	n
1302.17	2.75:	1.02	14
1304.86	5.54	2.17	15
1306.03	4.95	2.45	15
1641.30	17.26	8.96	16

5. The radial velocities

The orbital velocity of the B companion derived from optical measurements varies between -20 and $-40\ km\ s^{-1}$ (Wright, 1977), which, in the IUE spectral range, corresponds to shifts of 0.10 Å at 1500 Å and 0.20 Å at 3000 Å. It is therefore impossible to obtain reliable measurements of the orbital radial velocities from the IUE high resolution images.

However, we have measured the radial velocities of several lines of different ions in order to detect eventual systematic differences. The radial velocities for each image were measured independently by the three authors, both with a gaussian fit using the ELSPEC procedure (Pasian et al., 1984) and on the tracings, by measuring the line centers. The errors are obtained from the average of these measurements.

Since we do not have a constant radial velocity reference system, like that supplied by the interstellar lines, which in the case of VV Cep are not detectable, we have measured the radial velocity of various sets of lines in order to look for any systematic differences between such sets.

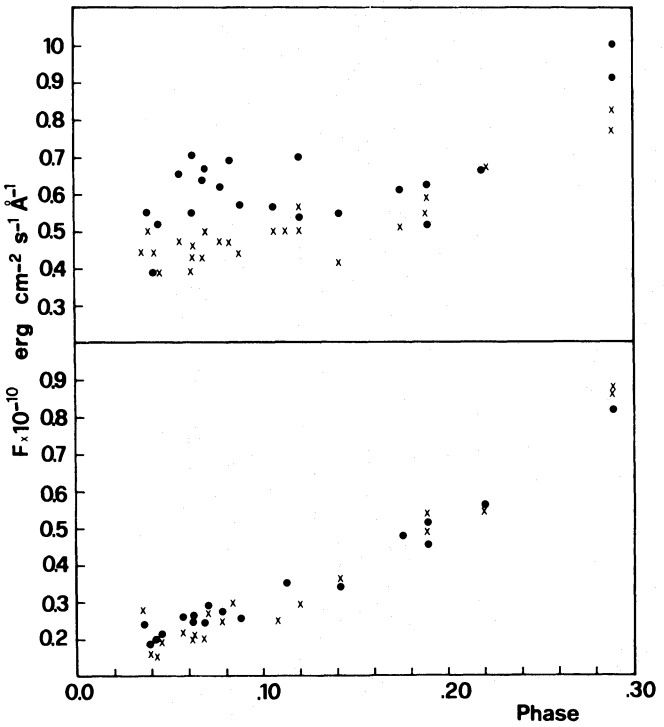

Fig. 8a. F_λ of the peak of the red emission wing of 2795 (●) and 2802 (×) Mg II versus the phase (top). The same for the violet emission wing (bottom)

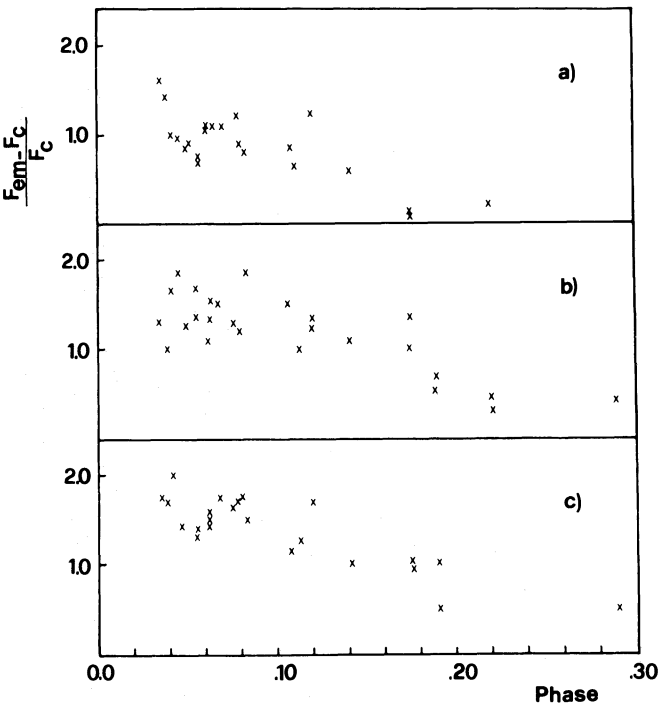

Fig. 9a–c. Central intensity $(F-F_c)/F_c$ versus the phase for the red (**a**) and violet (**b**) emission wings of 2756 Fe II, and for the central emission 2840 Fe II (**c**)

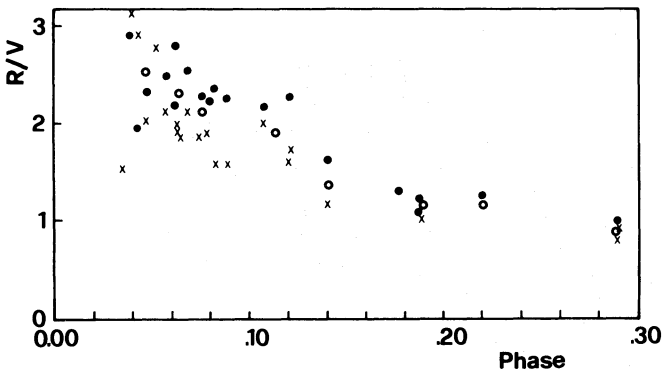

Fig. 8b. Ratio R/V for the emission wings of Mg II versus the phase: ● 2795, × 2802, ○ average values

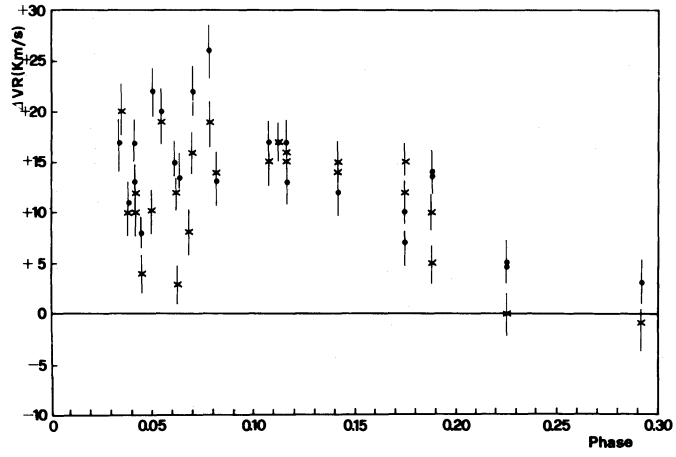

Fig. 10. Radial velocity differences versus the phase: (●) Mg I 2852 – average Fe II pure absorption lines in the near UV; (×) Fe II 2839 emission – average Fe II pure absorption lines in the near UV

The radial velocity of the 2852 Mg I absorption line, of the Mg II absorption cores of the resonance doublet and of the 2839 Fe II emission line minus the average velocity of the Fe II absorption lines are given in Figs. 10 and 11. The three plots show similar behaviors, the differences being of the order of about 10 km s^{-1} at phases 0.05–0.10 and systematically decreasing, reaching about zero at phases 0.20–0.30. Figure 12 shows the radial velocity of the absorption cores of the Fe II lines with emission wings minus the average radial velocity of the Fe II pure absorption lines, and the average radial velocity of the metallic ions V II and Ti II minus that of the Fe II absorption lines. Also in these cases small differences of +15 and −15 km s^{-1} respectively are observed at phases 0.05–0.10, tending to zero at phases 0.18–0.30.

In the far ultraviolet we have measured the radial velocity of the emission at 1641 O I] and that of the absorption cores of the Fe II lines of multiplet 191 relatively to the average radial velocity of the Fe II pure absorption lines (Fig. 13). In these cases, too, the differences are small, being about −25 km s^{-1} at phase 0.05 and

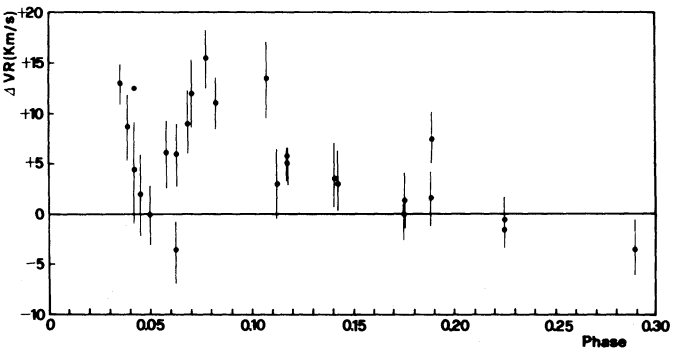

Fig. 11. The same as Fig. 10 for the average of the absorption cores of the two resonance lines of Mg II

Table 7. Multiplets of Fe II with emission lines and relative log *gf* (Kurucz, 1981), and related multiplets

Multiplet 391:	upper level e^4D – lower level z^4F
Line	log *gf*
2839.513	0.117 Emission
2848.320	−0.157 Doubtful
2851.723	−0.374 No
2865.459	−1.003 No
Multiplet 399:	upper level e^4D – lower level z^4D
Line	log *gf*
2845.596	0.008 Emission
2845.425	−0.624 Emission
2848.106	−0.288 Doubtful
2856.149	−1.090 No
Multiplet 363:	upper level e^6D – lower level z^6D
Line	log *gf*
2537.139	0.125 No
2530.103	−0.391 No
2525.919	−0.257 No
2550.152	−0.405 No
2538.680	−0.322 No
Multiplet 373:	upper level e^6D – lower level z^6F
Line	log *gf*
2767.512	0.090 No
2785.192	0.222 Emission
2754.884	−0.117 No
2776.908	−0.466 No
2762.333	−0.437 No
Multiplet 380:	upper level e^6D – lower level z^6P
Line	log *gf*
2839.800	−0.179 Blend with 2859.513
2856.377	−0.486 No
2833.086	−0.557 No

Table 7 (continued)

Multiplet 60:	upper level z^6F–lower level a^4D
Line	log *gf*
2926.585	−1.333 Absorption + two emission wings
2953.775	−1.417 Absorption + two emission wings
Multiplet 62:	upper level z^4F – lower level a^4D
Line	log *gf*
2755.737	0.425 Absorption + two emission wings
2749.321	0.319 Pure absorption
2746.484	0.157 Pure absorption
2743.197	−0.058 Pure absorption
Multiplet 63:	upper level z^4D – lower level a^4D
Line	log *gf*
2739.548	0.317 Pure absorption
2746.982	0.039 Pure absorption
Multiplet 64:	upper level z^4P – lower level a^4D
Line	log *gf*
2562.536	0.071 Pure absorption
2563.476	−0.215 Pure absorption
2582.584	−0.449 Pure absorption
Multiplet 78:	upper level z^4P – lower level a^4P
Line	log *gf*
3002.641	−0.016 Absorption + two emission wings
2984.825	−0.611 Absorption + two emission wings

decreasing regularly, approaching zero at phase 0.36. Figure 14 shows the radial velocity differences of the two pure emissions at 1641 O I] and 1869 Fe II and of the two violet emission wings of 1745 N I and 1785 Fe II, which again present the same behavior as that shown in Fig. 13.

In conclusion, these small but systematic differences in radial velocity suggest the presence of a slight stratification, which is more evident just after the end of the partial eclipse.

We have also attempted to measure the radial velocities of the broad strong resonance lines of C II, C IV, Si IV, Al II, Al III. However, they are too broad and blended; so the results are very uncertain and it is impossible to detect any variation with the phase. We give the average values over the whole observation period relatively to O I] 1641 (Table 8). In spite of the large errors, there is some evidence that these ions have a more positive velocity than 1641 O I].

Table 8. Radial velocity differences averaged over all the phases

Al II	1670	− [O I] 1641 =	+45 km s^{-1}	± 10 km s^{-1}
Al III	1854	− [O I] 1641 =	+8	± 9
Si IV	1393	− [O I] 1641 =	+32	±16
C IV	1548	− [O I] 1641 =	+74	±8

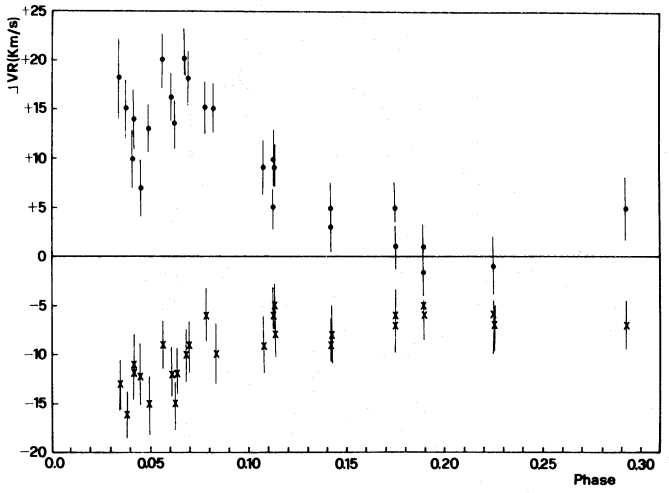

Fig. 12. The same as Fig. 10: × for the Fe II absorption cores of the lines with emission wings (in the near UV); ● for the average of the lines of Ti II and V II in the near UV

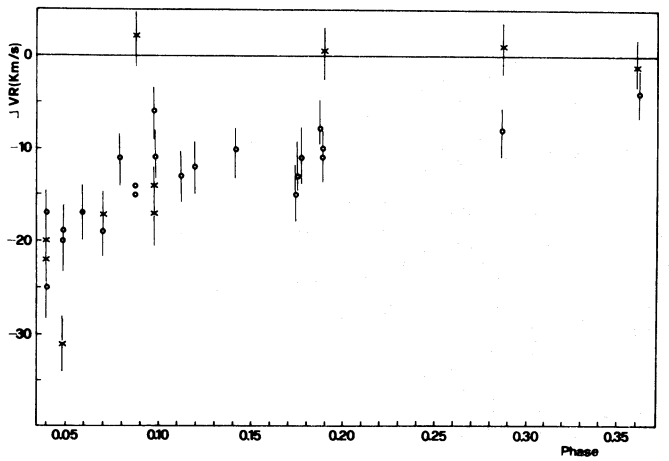

Fig. 13. Radial velocity differences versus the phase: o 1641 0 I] – average radial velocity of the pure absorption lines of Fe II and Ni II in the far UV; × the same for the absorption cores of the Fe II lines of multiplet 191

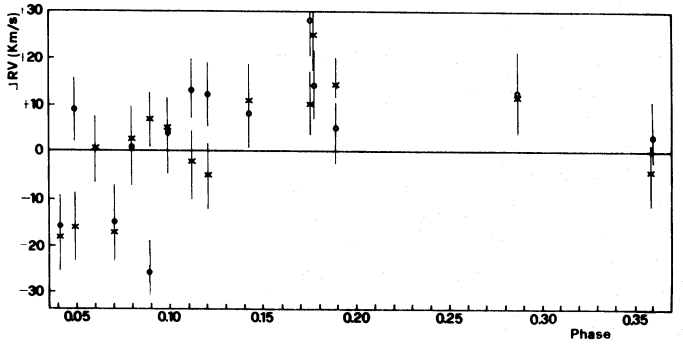

Fig. 14. Radial velocity differences versus the phase: o 1641 [0 I] emission – 1869 Fe II emission; × 1745 N I violet emission wing – 1785 Fe II violet emission wing

6. Conclusion

The study of the low and high resolution spectra of the atmospheric eclipsing binary VV Cep obtained with IUE after the fourth contact (from phase 0.04 to phase 0.36 counted from mid eclipse) has given the following results:

The interstellar reddening $E(B-V)=0.40$ is larger than that derived from optical observations. In spite of this rather large reddening, no interstellar lines are detectable, with the possible exception of the resonance lines of C I and O I.

The shorter the wavelength is, the later the epoch of the fourth contact.

The comparison of the UV energy distribution of VV Cep after the end of the eclipse with several standard stars observed with IUE, gives a spectral type A0 II for the companion.

In spite of the numerous and strong emissions observed in the optical, the ultraviolet spectrum is mainly an absorption line spectrum, with few moderately strong emissions of N I, O I, Mg II, Fe II and a rather weak Ly α.

The radial velocity differences of various sets of lines indicate slight systematic differences, diminishing as the phase increases.

Acknowledgements. We gratefully acknowledge the referee, Dr. A.K. Dupree, for several useful suggestions. We thank Mr. Loris Dilena who made the drawings.

References

Allen, C.W.: 1973, *Astrophysical Quantities*, Athlone Press, London
Elgaroy, O.: 1988, *Astron. Astrophys.* **204**, 147
Faraggiana, R., Selvelli, P.L.: 1979, *Astron. Astrophys.* **76**, L18
Hack, M., Selvelli, P.L.: 1982, *Astron. Astrophys.* **107**, 200
Hagen, W., Black, J.H., Dupree, A.K.: 1980, *Astrophys. J.* **238**, 203
Hummer, D.G.: 1968, *IAU Symposium* **34**, *Planetary Nebulae*, eds. D.E. Osterbrock, C.R. O'Dell, Reidel, Dordrecht, p. 166
Jamar, C., Macau-Hercot, D., Monfils, A., Thompson, G.I., Houziaux, L., Wilson, R.: 1976, ESA SR-27, Ultraviolet Bright-Star Spectrophotometric Catalogue
Johansson, S., Jordan, C.: 1984, *Monthly Notices Roy. Astron. Soc.* **210**, 239
Kalinowski, J.K.: 1983, *NASA Newsletter*, No. **22**, Nov. 4
Kelly, R.L.: 1987, *J. of Physical and Chemical Reference Data*, **16** *Suppl. No.* 1, *Atomic and Ionic Spectrum lines below* 2000 *Ångströms*
Kholopov, P.N.: 1985, *General Catalogue of Variable Stars*, Vol. I
Kurucz, R.L.: 1979, *Astrophys. J. Suppl.* **40**, 1
Kurucz, R.L.: 1981, *Smithsonian Astrophys. Obs. Spec. Rep.* **390**
Kurucz, R.L., Peytremann, E.: 1975, *Smithsonian Astrophys. Obs. Spec. Rep.* **362**
Osterbrok, D.E.: 1962, *Astrophys. J.* **135**, 195
Pasian, F., Rusconi, L., Sedmak, G.: 1984, *Publ. Astron. Obs. Trieste* No. **939**
Peery, B.F.: 1966, *Astrophys. J.* **144**, 672
Vladilo, G., Molaro, P., Crivellari, L., Foing, B.H., Beckmann, J.E., Genova, R.: 1987, *Astron. Astrophys.* **185**, 233
Wawrukiewicz, A. S., Lee, T.A.: 1974, *Publ. Astron. Soc. Pac.* **86**, 51
Weiler, E.J., Oegerle, W.R.: 1979, *Astrophys. J. Suppl.* **39**, 537
Wright, K.O.: 1977, *J. Roy. Astron. Soc. Canada* **71**, 152